Tutor/s

Dr. Eliana Ramírez Rangel
Department of Chemical Engineering/ Analytical Chemistry

Dr. Roger Bringué Tomàs
Department of Chemical Engineering/ Analytical Chemistry

Grau en Enginyeria Química

Treball Final de Grau

Preliminary kinetics study of 5-nonanol intramolecular dehydration over an acidic macroporous ion-exchange resin.

Víctor del Pozo Pòrtulas

June 2020

UNIVERSITAT DE BARCELONA

The most beautiful thing we can experience is the mysterious. It is the source of all true art and science.

Albert Einstein

En primer lloc voldria agrair als meus tutors, a l'Eliana Ramírez i al Roger Bringué, la seva paciència i ajuda incondicional en tot moment. També a tots els professors que he tingut a la carrera, per compartir els seus coneixements i aprendre de tots i cadascun d'ells.

A la meva família, per donar-me suport i per la confiança dipositada en mi des de que vaig començar la carrera, especialment als meus pares, a la meva germana i sobretot al meu tiet, qui sempre ha estat pendent de mi.

I finalment, als meus companys de promoció, per fer d'aquests quatre anys una experiència inoblidable i meravellosa.

CONTENTS

SUMMARY

The strong dependence on fossil fuels in our society is currently regarded as one of the most difficult problems to tackle in this era of huge energy demands. Possible solutions to replace these resources are being studied and one of them are biofuels. In order to obtain these products, a great reaction pathway must be carried out, where biomass-derived alkanoic acids coming from cellulose, hemicellulose, tall oil and vegetable oil, are converted into several valuable chemicals and motor fuel components.

The present work focusses on a certain reaction of this pathway, consisting of a 5-nonanol dehydration into 3-nonene and 4-nonene. A kinetic study has been carried out throughout experimental work in the laboratory. The main aim of this project is to find a kinetic equation that explains satisfactorily 5-nonanol dehydration over certain experimental conditions. Amberlyst-45 is used as catalyst because previous works confirm great results obtained with it.

To fulfill the objective, an extensive bibliographical research has been done to find the most common formulism to describe this type of reaction. Consequently, with all the information gathered, a total of 40 different expressions have been tested. Experimental data has been fitted to all of them. Selection of the best expression is based on four different parameters: Sum of square errors, residual distribution, evolution of the kinetic constant with temperature and activation energy. Two models provide good results in accordance with the parameters previously quoted. In the first one, based on Langmuir-Hinshelwood-Hougen-Watson formulism, an adsorbed molecule of 5-nonanol reacts to yield 3-nonene, 4-nonene and water. The equilibrium constant is considered to have a high value, which simplifies the final expression. The second model is based on Eley-Rideal formulism. Now, an adsorbed molecule of 5-nonanol reacts with another one in the bulk phase to yield 3-nonene, 4-nonene and water, which is released directly to solution. The equilibrium constant is considered to have a high value, as in the first model, and the adsorption term is simplified by suppressing the part corresponding to the desorption of 3-

nonene and 4-nonene. In both cases, reaction on the catalyst surface is considered as the rate controlling step of the process.

RESUM

La gran dependència que hi ha actualment cap als combustibles fòssils és considerat un dels problemes més difícils d'abordar en una era de grans requeriments energètiques. S'estan estudiant possibles solucions per substituir aquests recursos i una d'elles són els biofuels. Per tal d'obtenir aquests productes, cal dur a terme un conjunt de reaccions, on els àcids carboxílics derivats de la biomassa provinents de cel·lulosa, hemicel·lulosa, oli de pi i olis vegetals, són transformats en productes químics valuosos i components de combustibles de motors.

Aquest treball es centra en una reacció en concret, la qual consisteix en la deshidratació del 5-nonanol a 3-nonè i 4-nonè. S'ha efectuat un estudi cinètic a partir de treball experimental en el laboratori. L'objectiu principal d'aquest projecte és trobar una equació cinètica que expliqui satisfactòriament la deshidratació del 5-nonanol en unes condicions experimentals determinades. S'ha utilitzat Amberlyst-45 com a catalitzador, ja que en treballs anteriors s'han confirmat bons resultats amb el seu ús.

Per assolir l'objectiu principal, s'ha realitzat una extensa recerca bibliogràfica per trobar els formulismes més comuns que descriguin aquest tipus de reaccions. Conseqüentment, amb tota la informació reunida, s'han calculat un total de 40 expressions diferents. Totes s'han ajustat a dades experimentals. La selecció de la millor expressió es basa en quatre paràmetres: La suma dels error quadràtics, la distribució de residus, l'evolució de la constant cinètica amb la temperatura i l'energia d'activació. Hi ha dos models que aporten bons resultats segons els paràmetres anteriorment citats. En el primer, basat en el formulisme de Langmuir-Hinshelwood-Hougen-Watson, una molècula de 5-nonanol adsorbida reacciona per donar 3-nonè, 4-nonè i aigua. La constant d'equilibri es considera que té un valor molt elevat, la qual cosa simplifica l'expressió final. El segon model es basa en el formulisme Eley-Rideal. Una molècula de 5-nonanol adsorbida reacciona amb una altre que roman en la solució per donar 3-nonè, 4-nonè i aigua, la qual s'allibera directament en la solució. La constant d'equilibri es considera que té un valor molt elevat com en el primer model i el terme d'adsorció s'ha simplificat al suprimir la part

corresponent a la desorció del 3-nonè i 4-nonè. En ambdós casos, la reacció a la superfície del catalitzador es pren com a etapa controlant del procés.

Paraules clau: Biofuel, 5-nonanol, deshidratació, formulisme.

1. INTRODUCTION

1.1. PRODUCTION OF BIOFUELS

A future deprived from petroleum and the global warming affecting so dramatically our world makes us think about renewable fuels suitable enough, not only to progress as a society but also to improve our standard of life. A solution to this situation is liquid biofuels, proposed as the main source of energy due to its production from renewable biomass and low pollution generated when working with them. Biodiesel is one of the most widely used biofuels obtained from the esterification and transesterification of natural lipids such as vegetable oil or animal fats. Bioethanol is another important biofuel produced by the fermentation of sugars of some plants and, like biodiesel, both are based on technologies that have been studied in depth and are quite simple at the same time. There are basically two generations of biofuels considered as possible replacements of fossil fuels, both having several aspects to consider, not only in terms of yields but also in terms of global consensus.

First-generation biofuels, such as bioethanol and biodiesel, are suggested as a starting point in a chemical process [1] ,but they have some big downsides which removes them from the list of possible solutions. Firstly, they cannot satisfy such a huge demand, especially in the transportation sector. Secondly, they utilize edible biomass, which triggers an increase in the cost of food production and at the same time causes a competition for food sources.

The alternative to first-generation biofuels are second-generation biofuels, obtained from lignocellulosic biomass, which gives very useful compounds. The fact that second-generation biofuels do not have an impact on food industry makes them a suitable choice and the alternative to supply fossil fuels, even though they have some important drawbacks to bear in mind. They are limited to serving as blending agents, which makes petroleum alkenes still predominant in the fuel. Additionally, they suffer from low energy density and have limited applicability as jet or diesel fuel.

1.1.1. FROM BIOMASS TO LEVULINIC ACID

As it is said before, second-generation biofuels are the chosen ones to replace petroleum derived fuels, therefore it is been studied its conversion into useful platform chemicals like levulinic acid (LA), a five-carbon molecule with carboxylic acid and ketone functionalities, that enable interesting reactivity pathways. Identified by the US Department of Energy as one of the 12 most promising molecules derived from biomass, LA is a building block in the production of many biochemicals and has a potential industrial use as a plasticizer, animal feed or antifreeze. Some LA-derived products can be used for fuels as blenders in gasoline, diesel and jet fuel. Nevertheless, LA was not taken into consideration because of the high cost of raw material, the low yields obtained and the difficulty in separation and purification processes. As technology improved during the last decades, all these problems have been solved and LA has become one of the most important building blocks.

The process to obtain LA is illustrated in Figure 1 [2]. Vegetable biomass is used as a raw material but just a part of it (hemicellulose and especially cellulose) is useful to fulfil this goal. A complex reaction pathway is carried out, including a pretreatment due to lignocellulose recalcitrance, consistent on a hydrolyzation of cellulose into monosaccharides. The obtained glucose is isomerized to fructose, which is transformed into 5-hydroxymethylfurfural by dehydration. Finally, it is carried out a catalytical rehydration to form LA. The process of catalytical hydrolysis of cellulose has been studied worldwide during the last years, testing different acid catalysts with the purpose to get high yields. Heterogeneous catalysts were supposed to be a good option because of the easy recovery and tailorable properties but the fact is that yields
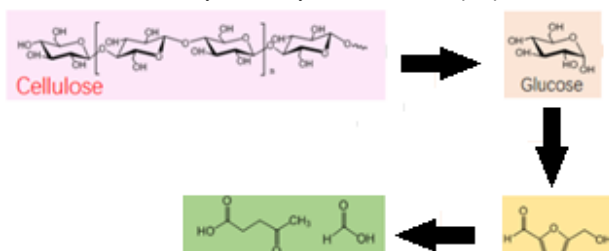

Figure 1: Process to obtain LA from the hydrosysis of cellulose. [2]

obtained were quite low [2]. Then, it was suggested to work with homogeneous acids due to the high process yields, but the problem now lies on the difficulty in recycling them. Nevertheless, toluene sulfonic acid (p-TsOH) was tested and results were surprisingly good [2]. Not only high

yields were obtained but also an easy recovery from the reaction, cooling the concentrated spent acid solution to ambient temperatures and reuse them.

Hemicellulose can be hydrolyzed into hexoses, which follow the same reaction pathway of glucose liberated from cellulose. In the future, it can be considered as an important alternative to obtain LA but nowadays it is not so studied as the process involving just cellulose.

LA is regarded as one of the most important platform chemicals due the wide range of possible value-added compounds that can be obtained from it. At the same time though, its high functionality turns out to be a downside because this makes it difficult to control its reactivity. This fact makes necessary a treatment based on a reduction of oxygen content in the molecule, leading to a less reactive intermediates that can be upgraded to the desired products [3].

1.1.2. FROM LA TO VALERIC ACID

Due to the cost-effective production proved by Biofine Corporation, LA is a great and economic platform chemical and nowadays is used worldwide. Many different compounds are derived from it such as alkyl levulinates and especially valeric acid (VA), also known as pentanoic acid (PA). This one, plays an important role in some steps of renewable fuels reaction pathway. Two different methodologies are proposed to obtain VA [4].

1.1.2.1. SINGLE STEP PROCESS

Figure 2 [4] shows how VA is produced using a single step process. There is a high selectivity towards VA when using Pt/HMFI as a catalyst and low pressures conditions of 0.5 MPa.
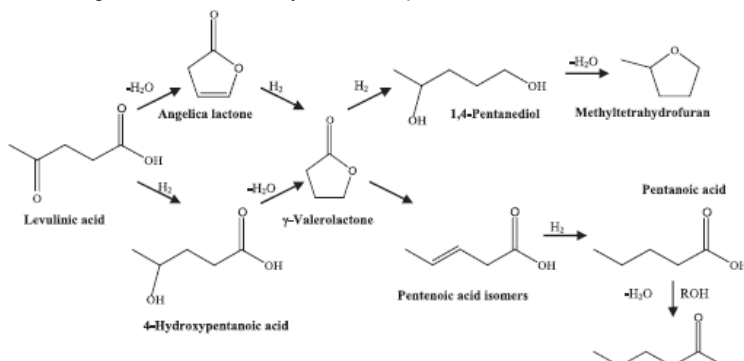

Figure 2: Single step process to obtain VA from LA. [4]

The first step consists in a hydrogenation on Pt sites of LA to Ɣ-valerolactone (GVL), which subsequently undergoes ring-opening on Bronsted acid sites of H-MFI to give an intermediate called pentenoic acid (PeA). Finally, PeA is hydrogenated on Pt sites to give VA.

Despite the fact of being an attractive solution due to its selectivity and simplicity, this alternative implies catalysts deactivation caused by carbon residue on the strong acid sites. Thus, a two-step process is much more successful [4].

1.1.2.2. TWO STEP PROCESS

Figure 3 [4] illustrates the steps followed to yield VA, showing each step and the compounds involved in it.
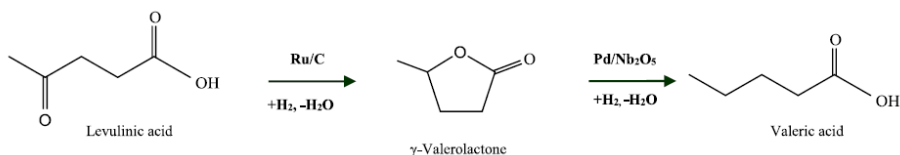

Figure 3: Two-step process to obtain VA from LA. [4]

This process does not suffer from catalyst deactivation and, unlike the previous one, there are two separately implemented transformations using in each one a different catalyst to carry out each process. Firstly, a continuous hydrogenation takes place over Ruthenia catalyst to produce GVL, which has excellent properties to be used as intermediate in chemical industry or for energy storage. The second stage consists of a combination of ring-opening over acid sites and hydrogenation reactions on metal sites using Pd/Nb_2O_5 catalyst [4].

Although two-step process has the highest yields and does not have problems of catalyst deactivation, CO_X is released as well. Nevertheless, just 5% of carbon is transformed into it, if the catalysts used are the ones named before. In addition, yields of 95% are achieved and VA is separated spontaneously from water, what makes it attractive in terms of purification [4].

1.1.3. FROM VALERIC ACID TO 5-NONANOL

Figure 4 [1] shows the whole pathway followed to obtain 5-nonanol (NOH) from VA and the different reactions involved in the process.
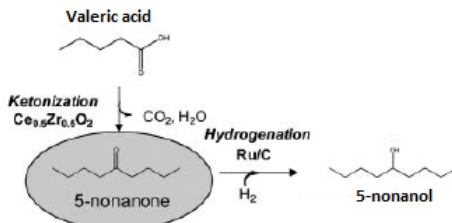
Figure 4:Process to upgrade GVL to liquid hydrocarbon fuels. [1]

According to literature [4], the most followed methodology to carry out this process, consists of two parts:

Firstly, carboxylic acids are coupled into high molecular weight compounds via ketonization on metal oxides. It has been proved, that systems based on zirconia are the most promising catalysts for the synthesis of ketones [4], presenting a high activity, being resistant to inhibition both by CO_2 as well as by water. They are also the most stable ones in comparison with others. Figure 5 [4] compares different catalysts used in this reaction and confirms this fact:
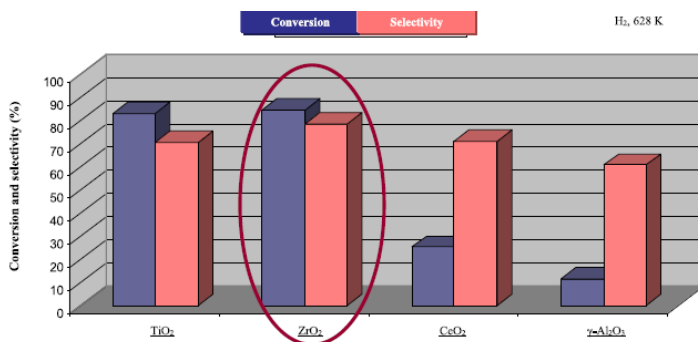
Figure 5: Catalytic properties of monometallic oxides in valeric acid ketonization. [4]

In addition, ketonization itself is a valuable way of lowering oxygen content. Thus, it is produced a less reactive intermediate that can be subsequently upgraded easier to the desired product. The second step consists of a hydrodeoxygenation of NOH with an adequate catalyst. Reduction of carbonyl group represents an important challenge. Thus, many works have been carried out to explain the mechanism, to find the best catalyst for this reaction [5] [6]. A very feasible option consists in using Ru/C as a catalyst at 423K, where conversions of nearly 100% and selectivity of 100% are achieved in 24h-30h of reaction. [1]

1.1.4. 5-NONANOL DEHYDRATION INTO NONENE

The current study focusses on this specific reaction, in which NOH is converted into various types of nonene (3-nonene and 4-nonene) by heterogenous catalysis. Alcohol dehydrations have been tested throughout the past years and have been also the subject of several previous studies [7]. Two possible mechanisms illustrated in figure 6 [7] are proposed to explain this process, both including protonation of hydroxyl group of the alcohol as the first step.
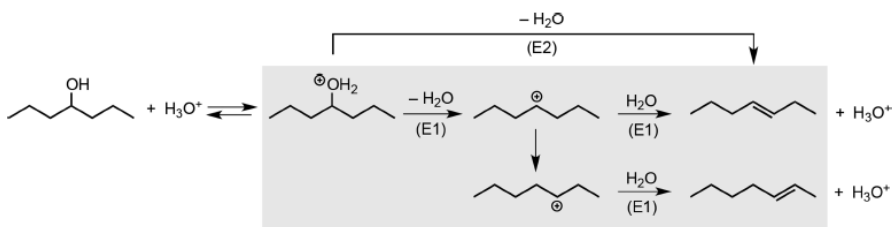

Figure 6: Processes (E1 and E2) proposed to explain alcohol dehydration. [7]

In E1 mechanism, the protonated oxygen leaves as a water molecule to generate an intermediate, that subsequently undergoes deprotonation, to finally form an alkene. Tertiary alcohols dehydrate usually via E1 mechanism because of the high stability of a more substituted cation when generating a tertiary carbocation intermediate. E2 mechanism is much faster because the loss of water and deprotonation occur simultaneously and there are no intermediates. This mechanism is predominant in primary alcohols due to a high instability of a hypothetical primary carbocation intermediate formed via E1 mechanism. For secondary alcohols, the mechanism is not so clear because there are no intuitive reasons, as in primary or tertiary alcohols, to claim if a certain mechanism is more plausible than another. Thus, it is thought that E1 and E2 are competitive to carry out the dehydration. According to literature [7], E1 mechanism is associated with negative entropy of activation whereas E2 mechanism is associated with positive entropy of activation. Therefore, dehydration of secondary alcohols is supposed to follow a pathway based on E1 mechanism. In some cases, it is quite accurate to propose a E2 mechanism when stereo electronic effects are favored, but at the same time, if a E1 mechanism is proposed, the results and yields obtained are quite similar. Therefore, in general it is accepted

a E1 mechanism to describe dehydration of secondary alcohols and consequently, to describe NOH dehydration.

To carry out NOH dehydration, an heterogenous catalysis is required, in which Amberlyst-45 (A45), a solid ion exchange resin, is used as a catalyst and NOH is the liquid reactant. Its kinetic modeling can reach a high level of complexity due to the several stages that take place throughout the reaction (external mass transfer, internal mass transfer, reagents adsorption, reaction on the surface of the catalyst and desorption of products). Any of these stages can determine the rate and the yield of the reaction. A proper choice of the catalyst can minimize their effect, then it is important to make emphasis in selecting the best possible one in accordance with the properties of the process.

1.1.4.1. CATALYST SELECTION

Once the liquid reactant has overcome internal and external mass transfer, the following step consists of an adsorption over a solid catalyst surface, which is the first important parameter to take into consideration, in terms of catalyst properties. A vast catalyst area is required to get reactants attached and consequently carry out all the steps of the process in the so-called active sites. Thus, porous solids are used as catalyst to have larger surface per mass unit. The area depends on the matrix, which is the main structure of the catalyst, acting as a framework, and it is made of long hydrocarbon chains by a cross-linking agent. A matrix must be stable enough to avoid changes when working in specific temperatures, pressures or in presence of certain substances that inhibit the catalyst. Its mechanical stability depends essentially on the synthesis methods employed. There are other important aspects to bear in mind, that are as much important as the number of active sites, such as the catalyst structure. This structure includes the catalyst diameter, which has a huge impact on internal mass transfer. To assess results obtained using a specific catalyst it is important to pay attention on its selectivity, activity and lifespan. In order to improve these features, it can be added some substances to the catalyst like chemical promoters. A low quantity of this can increase drastically the selectivity and the activity of the active sites of a certain catalyst.

There are several types of solid catalysts like zeolites or certain salts, but in this case, it has been chosen an ion exchange resin (A45 is the recommended one [8]). They can exchange ions with the medium in order to carry out the adsorption and desorption. Some of the advantages of

resins are its insolubility and mechanically stability. In addition, there are no problems of corrosion because most protons are inside the particle and waste treatment is much simpler due to the low levels of acidity or basicity of the waste products. Its density differs very little from that of organic solvents, thus it can be used in stirred tanks, remaining in suspension even at low stirring speeds. Besides, it can be used either in continuous or batch processes.

1.2. STATE-OF-THE-ART ALCOHOL DEHYDRATION KINETIC MODELS

Alcohol dehydrations have been studied throughout the years and there are many published papers [9] [10] [11] explaining these kinds of reaction extensively. Best conditions and catalysts are one of the interests of these studies, as well as kinetics. The latter is fulfilled by applying several formulism and fitting proposed models to experimental data. Langmuir-Hinshelwood-Hougen-Watson (LHHW) and Eley-Rideal (ER) formulisms are the most common ones used to describe heterogenous reactions at the surface of a solid catalyst. Molecules are absorbed on neighboring sites and a molecular reaction is undergone. In some cases, when inhibiting effects are present, empirical correlations are added like the coefficient of Freundlich [9] [10]. Some considerations are taken when using these formulisms:

- Catalyst surface contains a specific number of active sites.
- All active sites are identical.
- Reactivity of each active site depends only on temperature.

In literature it can be found studies of several alcohol kinetics, such as 1-Butanol dehydration [11]. In this case, Amberyst-70 is used as a catalyst at the temperature range of 413 K-473 K. Two models where regarded as suitable enough to explain the reaction. First of them consisted of a LHHW formulism, where two adjacent adsorbed molecules of 1-butanol reacted to yield ether and water, being reversible surface reaction, the rate limiting step (RLS) and considering adsorption of water negligible. The second one is also based on LHHW formulism but in this case the RLS is the desorption of water, considering the adsorption of ether negligible. In both previous cases, number of free active sites is found to be negligible in comparison with the occupied ones.

1-Pentanol papers have been revised as well [9]. In this case, the dehydration of this alcohol has been conducted using Amberylst-70 as catalyst again and at a range temperature of 423 K-463 K. Two suitable models were found to explain this reaction. On the one hand, a classical LHHW model very similar to the proposed one for 1-butanol, where two molecules of the alcohol

adsorbed on catalyst surface is considered the RLS. 1-Pentanol and water adsorption have an important contribution in the final equation. On the other hand, it is proposed an ER modified, where the surface reaction of one molecule of 1-pentanol from the bulk phase with one adsorbed 1-pentanol molecule is the RLS. Contribution of 1-pentanol adsorption into the final equation has a huge importance.

Finally, 1-octanol dehydration has been looked up too [10]. This reaction has been studied using once again Amberlyst-70 as catalyst and a temperature range of 413 K-453 K. Just one plausible model was proposed to describe this reaction, based on ER formulism. One molecule of 1-octanol adsorbed onto de resin reacts with another molecule of 1-octanol of the liquid phase. It is assumed that surface reaction is the RLS. 1-octanol and water adsorption play an important role in the final equation and the fraction of free active sites is negligible.

According to literature, it can be concluded that the most common RLS in alcohol dehydrations is the reaction on the surface and the number of free active sites is usually negligible.

2. OBJECTIVES

- Determine a kinetic equation that describes 5-nonanol dehydration over Amberlyst45, taking into consideration the different parts involved in the reaction and assuming the reaction on the catalyst surface as the rate controlling step. The selection of the best expression is based on the sum of square errors, residual distribution, evolution of the kinetic constant with temperature and the value of the activation energy.

- Carry out a bibliographic research about several alcohol dehydration to propose a model that describes 5-nonanol dehydration and apply certain simplifications to make the final equation simpler.

- Fit the proposed models to the experimental data to decide the one which explains better the reaction.

- Determination of the best model in accordance with the four parameters quoted and discussion of the influence of specific variables on the goodness of the fitting.

3. EXPERIMENTAL SECTION

When this work was firstly laid out, objectives involved in it where different from the current ones, therefore the initial plan had to be change due to the situation caused by COVID-19 pandemic.

The first objective consisted in determining the suitable condition of stirring speed and bead size to ensure that kinetic determinations were free from mass transfer resistances. All these experiments were planned to be conducted introducing the same amount of each reactants and catalyst inside the batch reactor:

- 45mL of 1,4-Dioxane (DI).
- 25mL of NOH.
- 2g of A45 (commercial size)

Thus, results obtained would not be disrupted because of the initial feed. In addition, the highest possible temperature was set in all these experiments (190ºC) to ensure that process was free from kinetic problems.

NOH is an expensive reactant which is sold in sets of 25 mL, but to conduct every experiment it is required a larger volume inside the reactor. Therefore DI, an inert specie in this reaction, is added to work with a suitable volume. DI is also used to ensure a monophasic system. Water, NOH and NO tend to form two phases, but the presence of DI solves this problem. Furthermore, liquid phase is ensured by stablishing a pressure of 25 bar in the system. In this condition, DI as well as NOH remains liquid and A45 is not affected at all.

Firstly, it was proposed to carry out NOH dehydration at a stirring speed range of 100rpm-700rpm until no changes were observed in the reaction rate. This fact would ensure that no external mass transfer problems had an influence in the reaction. Secondly, different bead size of Amberlyst-45 were supposed to be used in several experiments, once the suitable stirring speed was found. To do so and because of the wide distribution of particle diameter, the resin had to be firstly chopped and then sieved (at room temperature and humidity). Diameter of the

fraction selected varied from 0,4mm to 0,6mm and all of them had to be tested until no changes were observed in the kinetics of the reaction. Consequently, no internal mass transfer problems would affect to the reaction.

Once this aim was fulfilled, the second step consisted in carrying out more experiments at different temperatures, to obtain enough data to construct a kinetic model and find a kinetic equation that fits to experimental. It was planned to conduct the experiments at the temperature range of 140 ºC-190 ºC and at the same pressure of 25 bar explained previously.

Because of COVID-19 pandemic, just two months and a half were available to get used to the set up and to carry out a few experiments, like the ones to calibrate the chromatograph or some of them at different temperatures. Then, the project had to be changed and some objectives had to be suppressed. Fortunately, data from this specific reaction was available from another project and the results obtained from it are used to fulfill the objectives of the present work.

3.1. EXPERIMENTAL SET-UP

Figure 7 illustrates the necessary equipment to carry out all the experiments, pointing out the main elements.
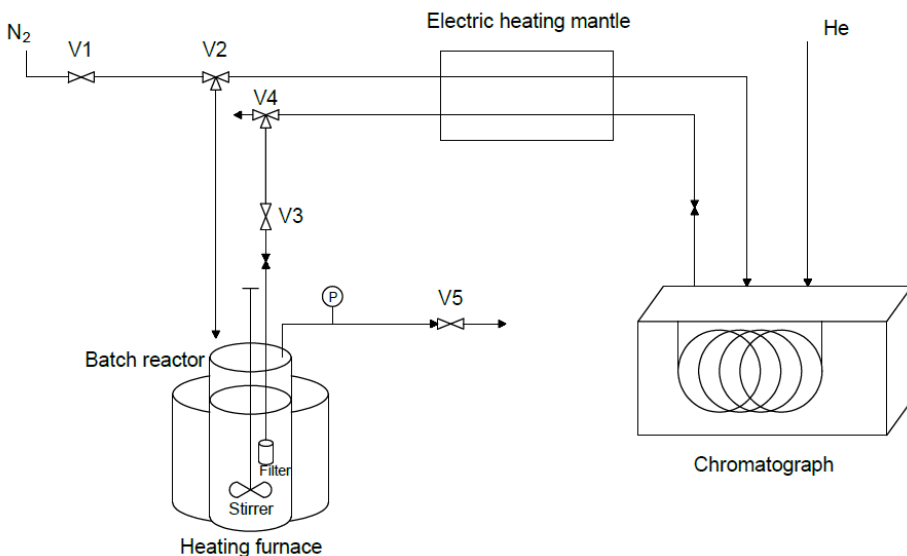

Figure 7: Experimental Set-up.

Both experiments and the calibration have been conducted at the same set up, composed principally of a 100mL autoclave batch reactor, whose operating pressure can be up to 25 bar and is measured using a manometer (Labon Druckmessumformer CB6020). There is a relief valve next to the manometer, which depressurize the system when necessary. This item is especially important when a sample is already analyzed by the chromatograph and it must be returned to the reactor. It is also useful to control pressure surges but in case of overpressurization, there is a rupture disk capable of resisting up to 54.8 bars with 5% error margin. The reactor has a stirring system composed of a four-paddle turbine mounted on a model Magnedrive II Series 0.7501 rotor. Depending on the stirring speed, which can be controlled by a frequency converter T-VERTER N2 SERIES, a vortex can be generated, affecting the results because of a bad mixing. That is why a baffle plate 316 SS is located alongside the turbine with the purpose to avoid this situation.

Each experiment has been carried out at a certain temperature, utilizing a heating furnace TC-22 Pro 9 controlled by a proportional integral derivative (PID) temperature control system. Measures have been done with a K type thermocouple. No sooner had the set-point been determined than the PID and the heating system proceed to achieve the stablished temperature with an error margin of ±0.1.

The reactor has an entrance of N_2 pushed inside by pneumatic transport, which allows the system to have such high pressures throughout the experiments. Connected to the reactor, a gas chromatograph runs a specific method to analyze samples.

3.2. EXPERIMENTAL PROCEDURE

3.2.1. CATALYST PRETREATMENT

A45 is a high-hydrophilic resin, which is sold with a high content of water. In order to remove it and conduct all the experiments correctly, it has been carried out a pretreatment to the ion-exchange resin. It is a time-consuming method that has been done the day before launching every single experiment and consists of two steps:

Firstly, a certain quantity of A45 is weighted using a scientific scale (4 decimal precision), usually two times more the amount of catalyst required for a certain experiment, and then it is put inside the atmospheric oven at a temperature of 110ºC for about 5h. It must be taken into consideration that 40%-50% of the whole weight is water.

Secondly, the resin is introduced to a vacuum oven at 110ºC and 10mbar throughout a whole night to remove as much water as possible (usually 3% of it remains in the resin). No sooner had the catalyst been taken out of it, than it is quickly weighted again to see how much dried A45 is available for the experiment. Then is kept in a closed box to prevent it from absorbing water from the atmosphere.

3.2.2. REACTOR LOADING

Both DI and NOH volumes are measured in a test tube and weighted on a scale to know exactly how much of each substance is used in every experiment. Then, the mixture is added inside the reactor alongside the amount of pretreated catalyst previously weighted. The volume

of the feeding mixture must not surpass 70% of the total volume of the batch reactor, therefore only 70mL have been introduced in each experiment. Afterwards, the reactor is screwed shut with three retaining screws to ensure a proper confinement and allow high pressures.

As soon as reactants and dioxane are loaded, valve V1 is opened and valve V2 is turned to position 1, with the aim of using all the N_2 gas to pressurize the batch reactor. At this point, the system has a pressure of 25 bar and the valve V1 is closed to check if there are any leaks by observing the manometer. If the tool gives a stable reading, then valve V1 is opened to make the next step. Otherwise, retaining screws and the other valves must be checked with the purpose to find a cause of this pressure fluctuation. In case everything is correct, the heating furnace is fastened around the reactor to clear the way for the start of the experiment.

3.2.3. EXPERIMENTAL LAUNCHING

Once the reactor loading is carried out properly, the stirring system, the temperature control system and the computer terminal are turned on. A specific set-point temperature inside the batch reactor is stablished in the electrical panel and a surface temperature set point of the heating furnace is programmed, 40ºC higher than the temperature inside the reactor. Afterwards, a certain mixing stirring, which depends on each experiment, is set with the frequency converter. A specific program is loaded to analyze the sample in the chromatograph. Right in this moment is considered the beginning of the experiment at time zero.

3.2.4. SAMPLING

At this point, everything is ready to take the first samples and obtain the first results. Valve V3 is opened while valve V4 remains in position 1, to allow the arrival of the sample to the chromatograph, which requires 2 minutes. Then button "START" is pressed to begin the analysis and after 30 seconds, the sample is returned to the reactor. To do so, it is necessary a lower pressure inside the reactor, which is achieved by opening valve V5. V2 must remain at the same time at position 2, blocking the entrance of N_2 gas that would increase the pressure and allowing the return of the sample. Valve V4 is turned to position 2 twice to purge the system and get it ready for another sampling within an hour. It is brought a pot near V4 to collect a quantity of sample, in the unlikely event it didn't return to the reactor. Finally, valve V2 is turned back to

position 1 to pressurize the system again. The system is purged once again by turning valve V4 several times to position 2. As mentioned before, this methodology is repeated at 1 h intervals.

4. RESULTS AND DISCUSSION

4.1. KINETIC MODELLING

The studied reaction is an heterogenous catalysis over A45 where NOH is dehydrated into different nonenes (4-nonene and 3-nonene), grouped as one specie called "nonene" (NO) for modelling purposes. According to results from laboratory, products obtained are just NO and water, therefore it has not been considered any other component, apart from the ones named before, when building the kinetic model. Reaction rate modelling consists of three different steps:

- Adsorption of NOH on A45 surface.
- Reaction on the surface of the catalyst.
- Desorption of the products.

I this model, kinetics is considered to be free from significant mass transfer resistances. Three models are proposed based on LHHW (the first one) formulism and ER formulism (the second and third one), depending on how many active sites interact throughout surface reaction [11] [9] [10].

4.1.1. LHHW MODEL PROPOSED

Figure 8 summarizes all the steps of the process according to the first model proposed, where σ corresponds to an active site, NOH to 5-nonanol, NO to 4-nonanone and W to water.
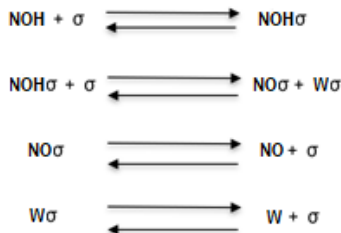

Figure 8: LHHW Mechanism proposed.

Chemical reaction on the surface of the catalyst is considered as the RLS of the process and consequently, adsorption of species is maintained in a quasi-equilibrium state all the time. This fact has a vast importance when finding the kinetic equation. According to Figure 8, NO as well as water remain absorbed on the catalyst, but there are other alternatives where NO or water are released into solution [11], as it will be explained later using an ER formulism. The main aim is to find an equation expressed as a combination of three different terms. Equation 1 shows the appearance of it:

$$r_P = \frac{(kinetic\ term) * (driving\ potential\ term)}{(absorption\ term)^n} \qquad (1)$$

Possible modifications on the equation can be found in the absorption term, like considering an amount of free active sites larger than the occupied ones. In this simple structure are included several parameters that will be fitted by calculating the sum of reaction rate square errors and making it minimum. The kinetic term includes all parameters related with reaction rate and some related with adsorption, depending on which rate controlling step is considered for a specific model. The driving potential term accounts for how far the thermodynamic equilibrium is, including the equilibrium constant of the process in liquid phase and concentrations of each component. This term becomes zero when the equilibrium is reached. The system deviates from ideality due to the important dissimilarity between compounds present on the medium. Instead of concentrations, the kinetic analysis has been carried out as a function of activities using the UNIFAC-Dortmund predictive method to estimate these activity coefficients [12] [13]. The adsorption term includes all parameters concerning the adsorption on catalyst surface, such as adsorption constants. In addition, the exponent "n" is the number of active sites in the step considered as the controlling one.

4.1.1.1. 5-NONANOL ADSORPTION

Reactants can be adsorbed in several different ways depending on how many molecules per active site take part in this stage. For example, many diatomic gases, such as hydrogen, interact with two active site and consequently, they dissociates in two different molecules, which remain at the catalyst surface [14]. Another type consists of the interaction of two molecules of reactant

with just one active site. In this case, a molecule of NOH is adsorbed in just one active site as it has been illustrated in Figure 8.

In order to study the adsorption rate, it is considered a simple adsorption model [14] in which a monomolecular layer over the catalyst surface is divided in two parts, a portion covered by NOH molecules and another part free from adsorbate. The problem is that concentrations on the surface cannot be measured and expressions relating these concentrations and the ones in the liquid phase will be needed to obtain a proper equation.

At a certain temperature, rate adsorption velocity is proportional to NOH concentration in the liquid phase (C_{NOH}) and empty sites concentration on catalyst surface (C'_V) the following way:

$$r'_{ads,NOH} = k_{a,NOH} * C_{NOH} * C'_v \qquad (2)$$

Where $k_{a,NOH}$ is the rate adsorption constant. At the same time, there is a desorption because there is an equilibrium. Desorption is proportional to the portion of surface catalyst covered by NOH, that is to say, it is proportional to the adsorbed NOH concentration (C'_{NOH}):

$$r'_{des,NOH} = k_{d,NOH} * C'_{NOH} \qquad (3)$$

Where $k_{d,NOH}$ is the rate desorption constant and C'_{NOH} is NOH concentration on the surface of catalyst. Combining equation (2) and (3) it can be obtained neat adsorption rate of NOH:

$$r'_{NOH} = k_{a,NOH} * C_{NOH} * C'_v - k_{d,NOH} * C'_{NOH} \qquad (4)$$

At the same time, it can be deduced adsorption equilibrium constant (K_{NOH}) combining both $k_{a,NOH}$ and $k_{d,NOH}$:

$$K_{NOH} = \frac{k_{a,NOH}}{k_{d,NOH}} \qquad (5)$$

The following expression is obtained by combining expression (4) and (5):

$$r'_{NOH} = k_{a,NOH} * \left(C_{NOH} * C'_V - \frac{C'_{NOH}}{K_{NOH}} \right) \tag{6}$$

4.1.1.2. CHEMICAL REACTION ON SURFACE CATALYST

Once NOH is adsorbed then starts the reaction in the active sites. Two products are released (water and NO), then it is necessary another active site, as shown in Figure 8, to carry out the reaction and consequently both products remain adsorbed in the active sites. Again, in this step there is an equilibrium, therefore the expression of it has the following appearance:

$$r_s = k' * C'_{NOH} * C'_V - k'' * C'_{NO} * C'_W \tag{7}$$

Where k' is the forward rate constant, k'' is the inverse rate constant, C'_{NO} is NO concentration on the surface of catalyst and C'_W is water concentration on surface catalyst too. Both constant can be combined as well, taking into consideration the rate equilibrium constant (K'):

$$K' = \frac{k'}{k''} \tag{8}$$

And again, combining both (7) as well as (8) the following equation is obtained:

$$r'_s = k' * \left(C_{NOH} * C'_V - \frac{C'_{NO} * C'_W}{K'} \right) \tag{9}$$

Expression (9) has a huge importance because of the fact of considering the reaction on catalyst surface as the RLS. Then, all the process has the rate expressed in this equation and the aim consist in finding expressions, to know concentrations of the components at the surface of the catalysts using different correlations, as done previously in the section before with NOH adsorption.

4.1.1.3. PRODUCTS DESORPTION

As shown in figure 8, there are two products obtained through this dehydration. In both cases it has been follow the same methodology to deduce rate desorption equations, just changing nomenclature using the suitable one. Thus, this section will be focused on just one product (nonene).

NO desorption equation can be easily deduced considering the same hypothesis explained on NOH desorption section, but now taking into consideration, that the process is the other way around, it consists of a desorption. Then it is obtained the following equations:

$$r'_{NO} = k_{d,NO} * C'_{NO} - k_{a,NO} * C_{NO} * C'_v \qquad (10)$$

$$K_P = \frac{k_{a,NO}}{k_{d,NO}} \qquad (11)$$

Where $k_{d,NO}$ is the rate desorption constant of NO, $k_{a,NO}$ the rate adsorption constant of NO and C_{NO} is NO concentration in the liquid face. Combining (10) and (11) it is obtained the following expression:

$$r'_{NO} = k_{a,NO} * \left(\frac{C'_{NO}}{K_{NO}} - C_{NO} * C_V' \right) \qquad (12)$$

It is followed the same steps to obtain rate desorption equation of water:

$$r'_W = k_{a,W} * \left(\frac{C'_W}{K_W} - C_W * C_V' \right) \qquad (13)$$

4.1.1.4. FINAL EQUATION

Once equations (6), (9), (12) and (13) are deduced, the following steps consists in putting together all of them in just one expression. Rate of the process is the one expressed by equation (9), because of the fact of considering it the RLS, thus, equation (6), (12) and (13) must be

implemented in it by considering them in a quasi-equilibrium state. Then, their rates are zero and it can be deduced the concentrations of each component on catalyst surface:

$$C'_{NOH} = K_{NOH} * C_{NOH} * C'_V \qquad (14)$$

$$C'_{NO} = K_{NO} * C_{NO} * C'_V \qquad (15)$$

$$C'_W = K_W * C_W * C'_V \qquad (16)$$

At the same time, it is known that the total number of active sites (C'_0) are either occupied by species of the process or are still free. Then the following equation is deduced:

$$C'_0 = C'_{NOH} + C'_W + C'_{NO} + C'_V \qquad (17)$$

This way, C'_V value can be calculated by substituting equation (14), (15) and (16) in equation (17):

$$C'_V = \frac{C'_0}{1 + K_{NOH} * C_{NOH} + K_{NO} * C_{NO} + K_W * C_W} \qquad (18)$$

Another important expression consists in combining all equilibrium constants and find a more simplified equation:

$$K = \frac{C_{NO} * C_W}{C_{NOH} *} * \frac{C'_{NOH} * C'_{NO} * C'_W * C'^2_V}{C'_{NOH} * C'_{NO} * C'_W * C'^2_V} = \frac{K_{NOH} * K'}{K_{NO} * K_W} \qquad (19)$$

At this point, all necessary calculations are done and now it is just a matter of adding equation (14), (15), (16), (18) and (19) into equation (9) to finally obtain the expression to describe the process properly:

$$r' = \frac{k' * K_{NOH} * C'_0{}^2 * \left(C_{NOH} - \frac{C_{NO} * C_W}{K}\right)}{(1 + K_{NOH} * C_{NOH} + K_{NO} * C_{NO} + K_W * C_W)^2} \qquad (20)$$

4.1.2. ER MODELS PROPOSED

ER formulism proposes a model where either water or nonene remained can be released into solution [11]. Consequently, the final equation is simpler than equation (20).

4.1.2.1. FIRST MODEL: NONENE REMAINS ADSORBED

Figure 9 summarizes all the steps of the process according ER formulism, where only one of the two reacting molecules of NOH is adsorbed yielding NO, that remains adsorbed on catalyst surface, and water, which is released into solution:
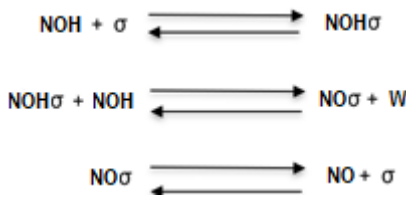

Figure 9: First ER mechanism proposed.

It has been followed the same steps of LHHW mechanism explained previously and the same hypothesis have been formulated, but all in accordance with ER formulism. Then, in this case, the final equation obtained is the next one:

$$r' = \frac{k' * K_{NOH} * C'_0 * \left(C_{NOH}{}^2 - \frac{C_{NO} * C_W}{K}\right)}{(1 + K_{NOH} * C_{NOH} + K_{NO} * C_{NO})} \qquad (21)$$

4.1.2.2. SECOND MODEL: WATER REMAINS ADSORBED

Figure 10 summarizes all the steps of the process according ER formulism, where only one of the two reacting molecules of NOH is adsorbed yielding water, that remains adsorbed on catalyst surface, and NO, which is released into solution:
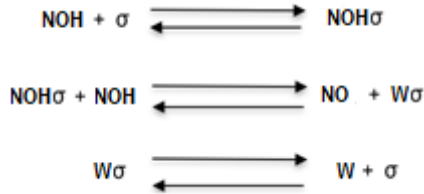

Figure 10:Second ER mechanism proposed.

As explained in the previous section, the methodology used to find a suitable expression that explains this process is the same used in LHHW formulism but adapted to this case. Then the equation obtained is the following one:

$$r' = \frac{k' * K_{NOH} * C'_0 * \left(C_{NOH}^2 - \frac{C_{NO} * C_W}{K}\right)}{(1 + K_{NOH} * C_{NOH} + K_W * C_W)} \tag{22}$$

As commented previously, several considerations can be estimated to make equation (20), (21) and (22) simpler and with less parameters to be fitted. Table 1 collects the main possible expressions according to each formulism. Simplifications are also applied based on considering the number of free active centers very low, in comparison with the occupied ones [11] [9]. Thus, the unit present in the denominator (the absorption term) can be removed. Other simplifications have been done like excluding a certain parameter of the equation to see if it is relevant or not. All the possibilities fitted (40 in total) can be found in annexes.

Table 1: All possible equations to describe 5-nonanol dehydration.

LHHW FORMULISM	
NO SIMPLIFICATION (LHHW1)	SIMPLIFICATION (LHHW2)
$$r' = \frac{k' * K_{NOH} * C'_0{}^2 * \left(a_{NOH} - \frac{a_{NO} * a_W}{K}\right)}{(1 + K_{NOH} * a_{NOH} + K_{NO} * a_{NO} + K_W * a_W)^2}$$	$$r' = \frac{k' * K_{NOH} * C'_0{}^2 * \left(a_{NOH} - \frac{a_{NO} * a_W}{K}\right)}{(K_{NOH} * a_{NOH} + K_{NO} * a_{NO} + K_W * a_W)^2}$$
ER FORMULISM (NONENE ADSORBED)	
NO SIMPLIFICATION (ER1)	SIMPLIFICATION (ER2)
$$r' = \frac{k' * K_{NOH} * C'_0 * \left(a_{NOH}{}^2 - \frac{a_{NO} * a_W}{K}\right)}{(1 + K_{NOH} * a_{NOH} + K_{NO} * a_{NO})}$$	$$r' = \frac{k' * K_{NOH} * C'_0 * \left(a_{N0H}{}^2 - \frac{a_{NO} * a_W}{K}\right)}{(K_{NOH} * a_{NOH} + K_{NO} * a_{NO})}$$
ER FORMULISM (WATER ADSORBED)	
NO SIMPLIFICATION (ER3)	SIMPLIFICATION (ER4)
$$r' = \frac{k' * K_{NOH} * C'_0 * \left(a_{NOH}{}^2 - \frac{a_{NO} * a_W}{K}\right)}{(1 + K_{NOH} * a_{NOH} + K_W * a_W)}$$	$$r' = \frac{k' * K_{NOH} * C'_0 * \left(a_{NOH}{}^2 - \frac{a_{NO} * a_W}{K}\right)}{(K_{NOH} * a_{NOH} + K_W * a_W)}$$

4.2. FITTING EXPERIMENTAL DATA AND SELECTION OF THE MODEL

Experimental data is used to fit all the parameters of the equations previously deduced. These parameters are the adsorption constants of each specie (K_{OH}, K_N and K_W), the equilibrium constant (K) and the kinetic constant (k'). Whenever possible, these constants have been grouped for mathematical purposes. As an example, equations 23 which corresponds to ER/2 formulism from Table 1, is modified including the associations mentioned. Expressions of each association are explained in equation 24 and 25.

$$r' = \frac{k_1 * \left(a_{N0H}^2 - \frac{a_{NO} * a_W}{K}\right)}{(a_{NOH} + K_1 * a_{NO})} \quad (23)$$

$$K_1 = \frac{K_{NO}}{K_{NOH}} \quad (24)$$

$$k_1 = \frac{k' * K_{NOH} * C'_0}{K_{NOH}} = k' * C'_0 \quad (25)$$

The sum of reaction rate square error (the squared difference between the experimental value and the calculated value) is minimized to find these parameters and determine which model fits better to experimental data. Residual distribution is taken into consideration too, when choosing the best model. This distribution should be random to regard a model as a suitable one, no tendency must be seen at all. Kinetic constant must increase with temperature all the time, otherwise, the model is not accepted. Finally, activation energy of the reaction has been calculated as well. Its value must be around 100 kJ/mol [9] [10] [11].

Mols from every specie and time are represented in four different graphs at four different temperatures using the experimental data (all at 500 rpm). An equation is fitted to the representations using the software "Curve Expert" by trying several mathematical models such as rational, logarithmic or exponential. Best results were obtained by representing a rational model expressed in equation 26:

$$n = \frac{(a + b * t)}{(1 + c * t + d * t^2)} \quad (26)$$

Where a,b,c and d are the four parameters adjusted at each temperature. Table 2 illustrates results obtained:

Table 2: Results obtained from fitting experimental data using Curve Expert.

T[ºC]	140	150	160	170
a	0,1214	0,1195	0,1199	0,1299
b	$-7,959 \cdot 10^{-7}$	$-1,126 \cdot 10^{-6}$	$-5,001 \cdot 10^{-6}$	$-7,024 \cdot 10^{-6}$
c	$1,343 \cdot 10^{-4}$	$2,689 \cdot 10^{-4}$	$3,753 \cdot 10^{-4}$	$1,227 \cdot 10^{-3}$
d	$9,978 \cdot 10^{-9}$	$1,229 \cdot 10^{-8}$	$1,625 \cdot 10^{-8}$	$3,317 \cdot 10^{-8}$

This type of mathematical model has been concluded as the best one because of the resemblance between the experimental graphs and the ones using the fitted parameters. Figure 11 shows how similar are both types of representations:
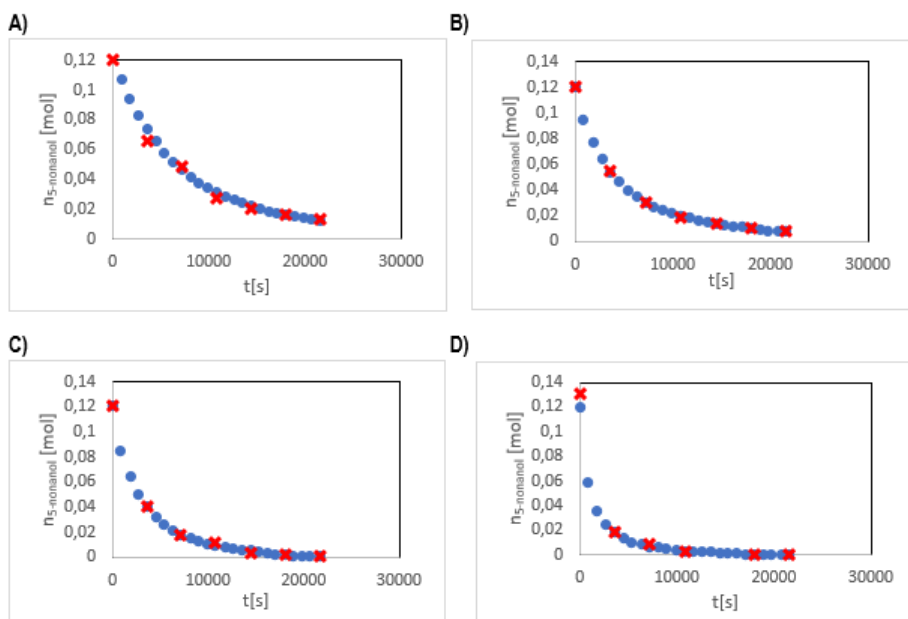

Figure 11: 5-nonanol mol vs time at (A) 140°C, (B) 150°C, (C)160°C and (D) 170°C. (●)fitted vàlues, (✱) experimental data.

Derivative of expression 26 is shown in equation 27 and corresponds to experimental reaction rate. Parameters from the models of Table 1 must be fitted using the values calculated with expression 27.

$$\frac{dn}{dt} = \frac{-b*d*x^2 - 2*a*d*x + b - a*c}{(1 + c*x + d*x^2)^2}$$

(27)

Theoretical reaction rate is calculated using all the models proposed. Surface rate constant and the adsorption equilibrium constants are dependent of temperature the following way:

$$K_i \text{ or } k' = A * exp\left\{(-B)*\left(\frac{1}{T} - \frac{1}{Tm}\right)\right\}$$

(28)

Where A and B are the factors that must be fitted with the experimental data, T is the temperature in each experiment and T_m corresponds to equation 29:

$$T_m = \frac{T_{min} + T_{max}}{2}$$

(29)

Models proposed form Table 1 have been modified by removing some terms in some cases from each equation. Thus, it is possible to see the effect of each constant and how good they fit to experimental. Table 3,5,6,7,8 and 9 gather all the 40 possibilities and they can be found in Appendix 1. As example, Table 3 shows all the possibilities applying a LHHW formulism without considering the number of active sites negligible. Each possibility corresponds to a certain letter (a, b, c, d, e, f, g, or h).

<div align="center">*Table 3: Possibilities from LHHW 1*</div>

	LHHW 1
a	$r' = (k' * K_{NOH} * C'^2_0 * (a_{NOH} - \{a_{NO} * a_W\}/K))/ (1 + K_{NOH} * a_{NOH} + K_{NO} * a_{NO} + K_W * a_W)^2$
b	$r' = (k' * K_{NOH} * C'^2_0 * a_{NOH})/ (1 + K_{NOH} * a_{NOH} + K_{NO} * a_{NO} + K_W * a_W)^2$
c	$r' = (k' * K_{NOH} * C'^2_0 * a_{NOH})/ (1 + K_{NO} * a_{NO} + K_W * a_W)^2$
d	$r' = (k' * K_{NOH} * C'^2_0 * a_{NOH})/ (1 + K_{NOH} * a_{NOH} + K_W * a_W)^2$
e	$r' = (k' * K_{NOH} * C'^2_0 * a_{NOH})/ (1 + K_{NOH} * a_{NOH} + K_{NO} * a_{NO})^2$
f	$r' = (k' * K_{NOH} * C'^2_0 * (a_{NOH} - \{a_{NO} * a_W\}/K))/ (1 + K_{NO} * a_{NO} + K_W * a_W)^2$
g	$r' = (k' * K_{NOH} * C'^2_0 * (a_{NOH} - \{a_{NO} * a_W\}/K))/ (1 + K_{NOH} * a_{NOH} + K_W * a_W)^2$
h	$r' = (k' * K_{NOH} * C'^2_0 * (a_{NOH} - \{a_{NO} * a_W\}/K))/ (1 + K_{NOH} * a_{NOH} + K_{NO} * a_{NO})^2$

4.2.1. BEST MODELS

Taking into consideration all the factors explained in the previous section, general models and the simplified ones have been fitted with all temperatures together. There are several kinetic models that explain satisfactorily NOH dehydration using A45 as catalyst. Some of them are better than others depending on the aspects explained in the previous section. Table 4 summarizes the main information from the best 3 models.

Table 4: Best kinetic models in accordance with the stablished criteria

ER4/b	
$$r' = \frac{k' * C'_0 * a_{NOH}^2}{\left(a_{NOH} + \frac{K_W}{K_{NOH}} * a_W\right)}$$	
ERROR: 0,059	Ea: 143,4kJ/mol
LHHW1/b	
$$r' = \frac{k' * K_{NOH} * C'^2_0 * a_{NOH}}{(1 + K_{NOH} * a_{NOH} + K_{NO} * a_{NO} + K_W * a_W)^2}$$	
ERROR:0,11	Ea: 83,14kJ/mol
ER1/d	
$$r' = \frac{k' * K_{NOH} * C'_0 * a_{NOH}^2}{(1 + K_{NOH} * a_{NOH})}$$	
ERROR: 0,18	Ea:109,1kJ/mol

The first model from Table 4 corresponds to ER formulism where water remains adsorbed and the fraction of active sites is negligible. The error is the lowest one but, as it can be seen in Figure 12, residual distribution is not random at all. In addition, activation energy is too high, which is an important drawback.
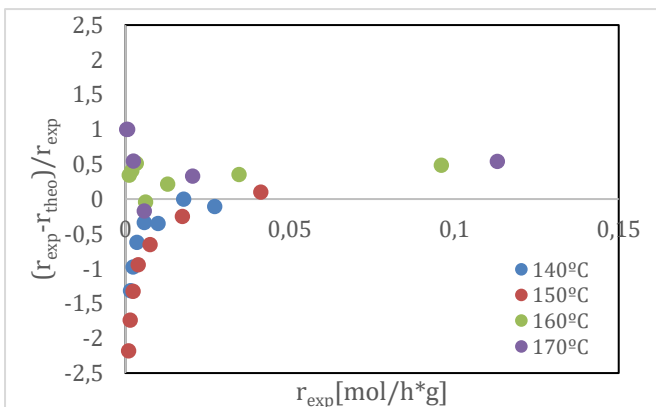

Figure 12: Residual distribution from ER4/b

On overall, models where the number of active sites is negligible do not provide good results. Activation energies are not close to 100kJ/mol, residual distribution is not random and in some of

them, kinetic constant does not increase as temperatures does. According to literature, best models are the ones, which take into consideration this simplification, but in this case, experimental conditions are different. In literature, all experiments were carried out starting with pure alcohol, but in this experimental work, the system is composed of NOH and DI. Then, not all active sites are occupied by the alcohol, but by DI too, making this simplification inadvisable.

All models from Table 4 have in common, that the equilibrium constant is considered to have a high value. Therefore, driving potential term is simplified and the equations have less parameters to be fitted. In general, best results amongst all 40 models proposed are obtained by applying this simplification, which corresponds to the fact that no equilibrium conditions were observed experimentally.

Second and third model from table 4 fit well to the studied reaction and the value of each constant can be found in Appendix 2. Both have activation energies close to 100kJ/mol and their errors are similar. In LHHW1/b, the activation energy is a little lower than the expected value. This fact could be caused because of internal and external mass transfer problems. As explained before, the suitable conditions to avoid these mass transfer resistances could not be found due to COVID-19 situation. Representations of experimental reaction rate against theoretical reaction rate and residual distribution of LHHW1/b and ER1/d are illustrated in Figure 13,14,15 and 16.
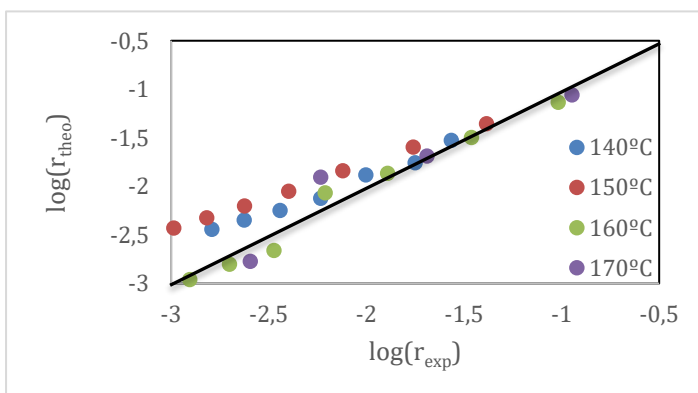

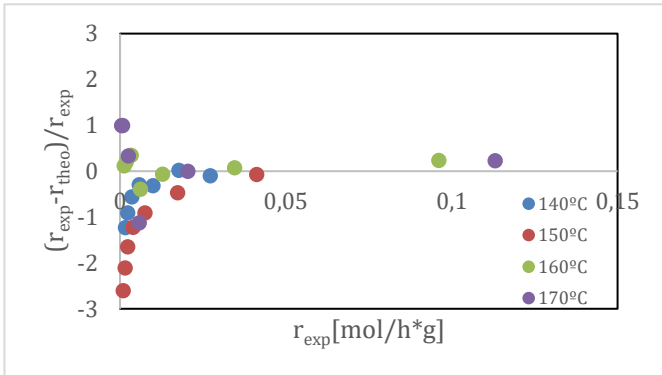*Figure 13: Logarith of theoretical reaction rate against logarithm of experimental rate for LHHW1/b*

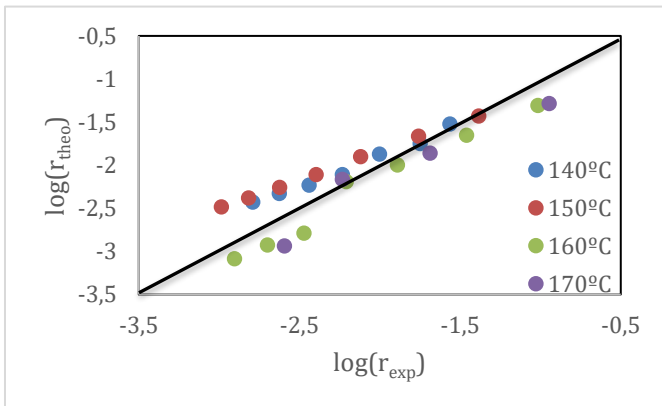*Figure 14:Residual distribution of LHHW1/b*

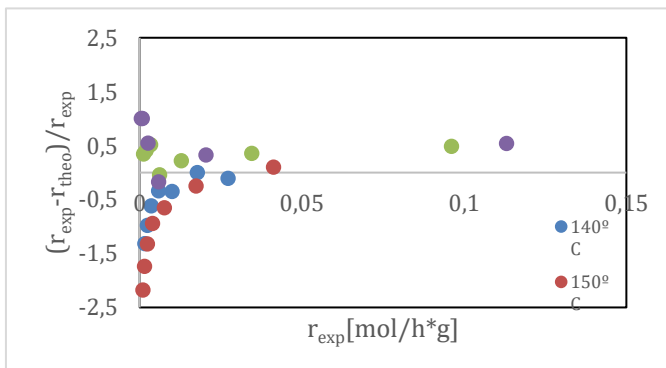*Figure 15: Logarith of theoretical reaction rate against logarithm of experimental rate for ER1/d*

Figure 16: Residual distribution of ER1/d

The evolution of the kinetic constant with the temperature can be seen in Figure 17 and 18:
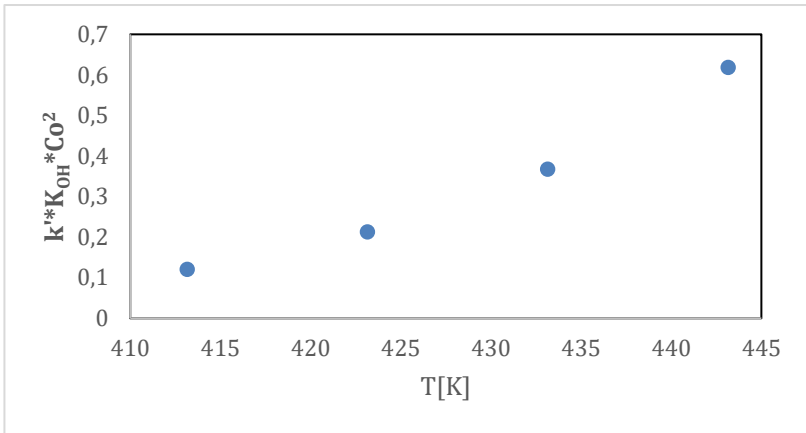
Figure 17: Evolution of k'*K_{OH}*$C_0{}^2$ with temperature for LHHW1/b
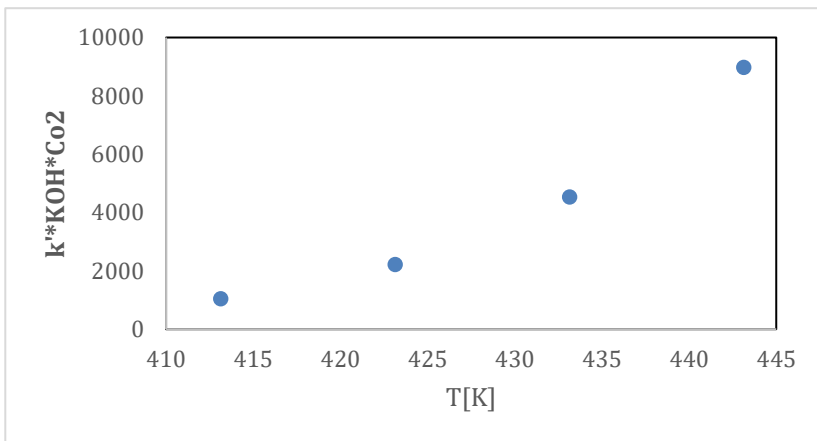
Figure 18: Evolution of k'*K_{OH}*$C_0{}^2$ with temperature for LHHW1/b

On the one hand, residual distributions in both cases are similar to ER4/b and it is not random. In general, no model has an absolute random residual representation, but models proposed in Table 4 are the closes ones to this type of distribution.

On the other hand, ER1/d has a lower error than LHHW1/b, but as commented before, ER1/d has a value of activation energy closer to the observed in the literature. In addition, in both cases,

the kinetic constant evolves with temperature as expected. In other cases, the value of k' remained constant with temperature, therefore these models had been excluded.

Although LHHW1/b as well as ER1/d have positive aspects such as the error obtained, the value of the activation energy and the evolution of the kinetic constant with temperature, their residual distribution is not random. At this point, there are no clear reasons to decide which model is better between ER1/d and LHHW1/b. To solve this problem, the range of concentrations of the experimental data should be enlarged by performing new tests at different NOH to DI ratios, adding nonene or water from the beginning or using different catalyst mass. Initially, this was the point of the present project, but the current situation deprived us to do so.

5. CONCLUSIONS

Once the project is done, the following conclusions can be extracted:

- To explain 5-nonanol dehydration over Amberlyst-45 to yield nonene and water, it has been used several models based on Langmuir-Hinshelwood-Hougen-Watson and Eley-Rideal formulism. Reaction on the catalyst surface is regarded as the rate controlling step and some simplifications have been applied like considering the number of active sites negligible.

- Two models, which stem from different mechanisms, have given the best results in accordance with the sum of square error obtained, residual distribution, evolution of the kinetic constant with temperature and the value of activation energy. In the first one, LHHW1/b, an adsorbed molecule of 5-nonanole reacts to yield nonene and water. The equilibrium constant is considered to have a high value. The second one, ER1/d, an adsorbed molecule of 5-nonanol reacts with another one in the bulk phase to yield nonene and water, which is released directly to solution. Equilibrium constant is considered to have a high value and the adsorption term is simplified by suppressing the term corresponding to the desorption of nonene.

- Energy activation of both models is close to the value expected from literature. Nevertheless, in LHHW1/b is lower, due to internal and external mass transfer problems.

- From these models, it is concluded that the number of active sites is not negligible because of the presence of DI in the reaction system. This causes bad results when fitting experimental data. In addition, 5-nonanol dehydration is not an equilibrium reaction because of the high value of the equilibrium constant.

- It is not possible to discern between LHHW1/b and ER1/d model due to the lack of experiments at different conditions of initial reactant ratios and mass of catalyst used.

REFERENCES AND NOTES

[1] D. M. Alonso, J. Q. Bond, J. C. Serrano-Ruiz and J. A. Dumesic, "Production of liquid hydrocarbon transportation fuels by oligomerization of biomass-derived C 9 alkenes.," Green chemistry, vol. 12, no. 6, pp. 992-999, 2010.

[2] H. Ji, C. Dong, G. Yang and Z. Pang, "Production of levulinic acid from lignocellulosic biomass with a recyclable aromatic acid and its kinetic study.," BioResources, vol. 14, no. 1, pp. 725-736, 2019.

[3] J. C. Serrano-Ruiz, D. Wang and J. A. Dumesic, "Catalytic upgrading of levulinic acid to 5-nonanone.," Green Chemistry, vol. 12, no. 4, pp. 574-577, 2010.

[4] I. L. Simakova and D. Y. & Murzin, "Transformation of bio-derived acids into fuel-like alkanes via ketonic decarboxylation and hydrodeoxygenation: Design of multifunctional catalyst, kinetic and mechanistic aspects.," Journal of Energy Chemistry, vol. 25, no. 2, pp. 208-224, 2016.

[5] A. Farkas and L. & Farkas, "The Catalytic Interaction of Acetone and Isopropyl Alcohol with Deuterium on Platinum.," Journal of the American Chemical Society, vol. 61, no. 6, pp. 1336-1341, 1939.

[6] L. C. Anderson and N. W. & MacNaughton, "The Mechanism of the Catalytic Reduction of Some Carbonyl Compounds1.," Journal of the American Chemical Society, vol. 64, no. 6, pp. 1456-1459, 1942.

[7] C. Bockisch, E. D. Lorance, H. E. Hartnett, E. L. Shock and I. R. Gould, "Kinetics and mechanisms of dehydration of secondary alcohols under hydrothermal conditions.," ACS Earth and Space Chemistry, vol. 2, no. 8, pp. 821-832, 2018.

[8] D. M. Alonso and J. Q. &. D. J. A. Bond, "Catalytic conversion of biomass to biofuels," Green chemistry, vol. 12, no. 9, pp. 1493-1513, 2010.

[9] R. Bringué, E. Ramírez, C. Fité, M. Iborra and J. Tejero, "Kinetics of 1-pentanol etherification without water removal.," Industrial & engineering chemistry research, vol. 50, no. 3, pp. 7911-7919, 2011.

[10] C. B. R. F. C. I. M. &. T. J. Casas, "Kinetics of the liquid phase dehydration of 1-octanol to di-n-octyl ether on Amberlyst 70.," AIChE Journal, vol. 63, no. 9, pp. 3966-3978, 2017.

[11] M. Á. Pérez-Maciá, R. Bringué, M. Iborra, J. Tejero and F. Cunill, "Kinetic study of 1-butanol dehydration to di-n-butyl ether over Amberlyst 70.," AIChE Journal, vol. 62, no. 1, pp. 180-194, 2016.

[12] B. E. Poling, J. M. Prausnitz and J. P. O'connell, The properties of gases and liquids, New York: Mcgraw-hill, 2001.

[13] A. Fredenslund, R. L. Jones and J. M. Prausnitz, "Group-contribution estimation of activity coefficients in nonideal liquid mixtures.," AIChE Journal, vol. 21, no. 6, pp. 1086-1099, 1975.

[14] J. F. Izquierdo, F. Cunill, J. Tejero, M. Iborra and C. Fité, Cinética de las reacciones químicas, Barcelona: Ediciones Universitat Barcelona, 2004.

[15] D. J. Hayes, S. Fitzpatrick, M. H. Hayes and J. R. Ross, "The biofine process–production of levulinic acid, furfural, and formic acid from lignocellulosic feedstocks.," Biorefineries– Industrial Processes and Product, vol. 1, pp. 139-164, 2006.

[16] A. de Klerk, "Oligomerization of 1-hexene and 1-octene over solid acid catalysts.," Industrial & engineering chemistry research, vol. 44, no. 11, pp. 3887-3893, 2005.

[17] J. P. Pater, P. A. Jacobs and J. A. Martens, "1-hexene oligomerization in liquid, vapor, and supercritical phases over beidellite and ultrastable Y zeolite catalysts.," Journal of catalysis, vol. 179, no. 2, pp. 477-482, 1998.

[18] R. J. Quann, L. A. Green, S. A. Tabak and F. J. Krambeck, "Chemistry of olefin oligomerization over ZSM-5 catalyst.," Industrial & engineering chemistry research, vol. 27, no. 4, pp. 565-570, 1988.

ACRONYMS

LA: Levulinic acid.

VA: Valeric acid.

PA: Pentanoic acid.

GVL: ϒ-valerolactone.

PeA: Pentenoic acid.

NOH: 5-nonanol.

NO: Nonene.

A45: Amberlyst-45.

LHHW: Langmuir-Hinshelwood-Hougen-Watson.

ER: Eley-Rideal.

RLS: Rate limiting step.

DI: 1,4-Dioxane.

APPENDICES

APPENDIX 1: ALL MODELS TESTED.

Table 3: Possibilities from LHHW 1

LHHW 1	
a	$r' = (k' * K_{NOH} * C'^2_0 * (a_{NOH} - \{a_{NO} * a_W\}/K))/ (1 + K_{NOH} * a_{NOH} + K_{NO} * a_{NO} + K_W * a_W)^2$
b	$r' = (k' * K_{NOH} * C'^2_0 * a_{NOH})/ (1 + K_{NOH} * a_{NOH} + K_{NO} * a_{NO} + K_W * a_W)^2$
c	$r' = (k' * K_{NOH} * C'^2_0 * a_{NOH})/ (1 + K_{NO} * a_{NO} + K_W * a_W)^2$
d	$r' = (k' * K_{NOH} * C'^2_0 * a_{NOH})/ (1 + K_{NOH} * a_{NOH} + K_W * a_W)^2$
e	$r' = (k' * K_{NOH} * C'^2_0 * a_{NOH})/ (1 + K_{NOH} * a_{NOH} + K_{NO} * a_{NO})^2$
f	$r' = (k' * K_{NOH} * C'^2_0 * (a_{NOH} - \{a_{NO} * a_W\}/K))/ (1 + K_{NO} * a_{NO} + K_W * a_W)^2$
g	$r' = (k' * K_{NOH} * C'^2_0 * (a_{NOH} - \{a_{NO} * a_W\}/K))/ (1 + K_{NOH} * a_{NOH} + K_W * a_W)^2$
h	$r' = (k' * K_{NOH} * C'^2_0 * (a_{NOH} - \{a_{NO} * a_W\}/K))/ (1 + K_{NOH} * a_{NOH} + K_{NO} * a_{NO})^2$

Table 5:Possibilities from LHHW 2

	LHHW 2
a	$r' = (k' * C'^2_0 * (a_{NOH} - \{a_N * a_W\}/K))/ (a_{NOH} + (K_{NO}/K_{OH}) * a_N + (K_W/K_{OH}) * a_W)^2$
b	$r' = (k' * C'^2_0 * a_{NOH})/ (a_{NOH} + (K_{NO}/K_{OH}) * a_N + (K_W/K_{OH}) * a_W)^2$
c	$r' = (k' * K_{NOH} * C'^2_0 * a_{NOH})/ (K_{NO} * a_{NO} + K_W * a_W)^2$
d	$r' = (k' * C'^2_0 * a_{NOH})/ (a_{NOH} + (K_W/K_{OH}) * a_W)^2$
e	$r' = (k' * C'^2_0 * a_{NOH})/ (a_{NOH} + (K_{NO}/K_{OH}) * a_N)^2$
f	$r' = (k' * K_{OH} * C'^2_0 * (a_{OH} - \{a_N * a_W\}/K))/ (K_N * a_N + K_W * a_W)^2$
g	$r' = (k' * C'^2_0 * (a_{NOH} - \{a_N * a_W\}/K))/ (a_{NOH} + (K_W/K_{OH}) * a_W)^2$
h	$r' = (k' * C'^2_0 * (a_{NOH} - \{a_N * a_W\}/K))/ (a_{NOH} + (K_{NO}/K_{OH}) * a_N)^2$

Table 6:Possibilities from ER 1.

	ER 1
a	$r' = (k' * K_{NOH} * C'_0 * (a^2_{NOH} - \{a_{NO} * a_W\}/K))/(1 + K_{NOH} * a_{NOH} + K_{NO} * a_{NO})$
b	$r' = (k' * K_{NOH} * C'_0 * a^2_{NOH})/(1 + K_{NOH} * a_{NOH} + K_{NO} * a_{NO})$
c	$r' = (k' * K_{NOH} * C'_0 * a^2_{NOH})/(1 + K_{NO} * a_{NO})$
d	$r' = (k' * K_{NOH} * C'_0 * a^2_{NOH})/(1 + K_{NOH} * a_{NOH})$
e	$r' = (k' * K_{NOH} * C'_0 * (a^2_{NOH} - \{a_{NO} * a_W\}/K))/(1 + K_{NO} * a_{NO})$
f	$r' = (k' * K_{NOH} * C'_0 * (a^2_{NOH} - \{a_{NO} * a_W\}/K))/(1 + K_{NOH} * a_{NOH})$

Table 7: Possibilities from ER 2.

	ER 2
a	$r' = (k' * C'_0 * (a_{NOH}^2 - \{a_{NO} * a_W\}/K))/(a_{NOH} + (K_{NO}/K_{NOH}) * a_{NO})$
b	$r' = (k' * C'_0 * a_{NOH}^2)/(a_{NOH} + (K_{NO}/K_{NOH}) * a_{NO})$
c	$r' = (k' * K_{NOH} * C'_0 * a_{NOH}^2)/(K_{NO} * a_{NO})$
d	$r' = k' * C'_0 * a_{NOH}$
e	$r' = (k' * K_{NOH} * C'_0 * (a_{NOH}^2 - \{a_{NO} * a_W\}/K))/(K_{NO} * a_{NO})$
f	$r' = (k' * C'_0 * (a_{NOH}^2 - \{a_{NO} * a_W\}/K))/a_{NOH}$

Table 8: Possibilities from ER 3.

	ER 3
a	$r' = (k' * K_{NOH} * C'_0 * (a_{NOH}^2 - \{a_{NO} * a_W\}/K))/(1 + K_{NOH} * a_{NOH} + K_W * a_W)$
b	$r' = (k' * K_{NOH} * C'_0 * a_{NOH}^2)/(1 + K_{NOH} * a_{NOH} + K_W * a_W)$
c	$r' = (k' * K_{NOH} * C'_0 * a_{NOH}^2)/(1 + K_W * a_W)$
d	$r' = (k' * K_{NOH} * C'_0 * a_{NOH}^2)/(1 + K_{NOH} * a_{NOH})$
e	$r' = (k' * K_{NOH} * C'_0 * (a_{NOH}^2 - \{a_{NO} * a_W\}/K))/(1 + K_W * a_W)$
f	$r' = (k' * K_{NOH} * C'_0 * (a_{NOH}^2 - \{a_{NO} * a_W\}/K))/(1 + K_{NOH} * a_{NOH})$

Table 9: Possibilities from ER 4.

ER 4	
a	$r' = (k' * C'_0 * (a_{NOH}^2 - \{a_{NO} * a_W\}/K))/(a_{NOH} + (K_W/K_{OH}) * a_W)$
b	$r' = (k' * C'_0 * a_{NOH}^2)/(a_{NOH} + (K_W/K_{OH}) * a_W)$
c	$r' = (k' * K_{NOH} * C'_0 * a_{NOH}^2)/(K_W * a_W)$
d	$r' = (k' * C'_0 * a_{NOH})$
e	$r' = (k' * K_{NOH} * C'_0 * (a_{NOH}^2 - \{a_{NO} * a_W\}/K))/(K_W * a_W)$
f	$r' = (k' * C'_0 * (a_{NOH}^2 - \{a_{NO} * a_W\}/K))/(a_{NOH})$

APPENDIX 2: VALUES FROM THE BEST MODELS.

Table 10: Results from LHHW1/b obtained.

T[K]	$k'*K_{NOH}*C_0^2$	K_{NOH}	K_{NO}	K_W
413,15	0,120	0	0	0,220
423,15	0,213	0	0	0,390
433,15	0,367	0	0	0,673
443,15	0,618	0	0	1,134

Table11: Results from ER1/d

T[K]	$k'*K_{NOH}*C_0^2$	K_{NOH}	K_{NO}
413,15	1045,194	8684,00555	0
423,15	2213,945	12873,2276	0
433,15	4529,870	18739,6148	0
443,15	8973,718	26820,9493	0